



Original Research

Adipose-Derived Stem Cells Transfected to Express Brain-Derived Neurotrophic Factor Reduce Hippocampal Amyloid Plaque Load and Improve Dendritic Morphology in the APP/PS1dE9 Mouse Model of Alzheimer's Disease

Yuzhen Luo^{1,†}, Yiheng Liu^{2,†}, Hui Long¹, Caini Pei¹, Lujia Mao¹,
Gregory M. Rose³, Haiying Zhang^{1,4,*}

¹Hainan Province Key Laboratory of Brain Science and Health Translational Medicine Research Center in Tropical Environment, Hainan Medical University (Hainan Academy of Medical Science), 571199 Haikou, Hainan, China

²Department of Orthopedic, Affiliated Haikou Hospital of Xiangya Medical College, Central South University, 571199 Haikou, Hainan, China

³Department of Anatomy, School of Medicine, Southern Illinois University, Carbondale, IL 62901, USA

⁴Hainan Provincial Key Laboratory of Carcinogenesis and Intervention, Hainan Medical University, 571199 Haikou, Hainan, China

*Correspondence: hy0206102@hainmc.edu.cn (Haiying Zhang)

†These authors contributed equally.

Academic Editors: Hongmin Wang and Bettina Platt

Submitted: 26 August 2025 Revised: 14 November 2025 Accepted: 3 December 2025 Published: 23 January 2026

Abstract

Background: Recent studies have indicated that stem cells could provide therapeutic benefits in several neurological conditions, including Alzheimer's disease (AD). Adipose-derived stem cells (ADSCs) offer many advantages in that they are readily available from individual hosts, are robust, and secrete many factors that promote neuronal growth and homeostasis. **Methods:** We transfected ADSCs with a viral construct for brain-derived neurotrophic factor (BDNF) and examined the effects of transplanting these cells into the hippocampus of 7-mo-old APPswe/PS1dE9 mice. After 6 mo, the hippocampus was examined for stem-cell survival, effects on BDNF and neprilysin-2 (NEP-2) levels, dendritic morphology using microtubule associated protein 2 (MAP2) immunohistochemistry, and amyloid plaque load. **Results:** We found that transplanted BDNF-ADSCs had survived after 6 mo. BDNF and NEP-2 levels were higher than sham controls, and dendritic architecture was improved. In addition, amyloid plaque numbers were reduced. **Conclusions:** BDNF-ADSCs appear to confer benefits by simultaneously enhancing amyloid clearance and promoting neuronal structural repair. This multifaceted approach highlights the potential of engineering stem cells to target multiple pathophysiological hallmarks of AD, positioning BDNF-ADSCs as a powerful and synergistic cell-gene therapy strategy for this devastating disorder.

Keywords: adipose tissue; Alzheimer's disease; brain-derived neurotrophic factor; hippocampus; mesenchymal stem cells

1. Introduction

Alzheimer's disease (AD) is the predominant neurodegenerative disorder, with a profound impact on millions of elderly people across the globe [1]. AD is characterized by extracellular β -amyloid plaques and intracellular neurofibrillary tangles. These pathologies collectively trigger synaptic dysfunction and neuronal loss in the brain [2]. Despite considerable endeavors, current therapeutic strategies, focused largely on symptomatic relief and cognitive improvement, have yielded limited and merely transient benefits [3].

Propelled by recent progress, stem-cell technology holds significant promise for generating innovative therapeutic interventions for neurodegenerative disorders [4–6]. Under appropriate inductive conditions, adipose-derived stem cells (ADSCs) undergo differentiation into cells that express established neuronal and glial protein markers, in addition to their inherent high proliferative potential *in vitro* [7]. Further, it has been shown that intracerebral adminis-

tration of ADSCs reduced pathology and memory impairments in mouse models of AD [8–11]. The clinical translation of ADSCs for neurological disorders is constrained by critical limitations, including uncertain efficacy, poor long-term survival after transplantation, and inefficient homing to target brain areas. These challenges hinder the reliability and therapeutic potential of ADSC-based approaches. Brain-derived neurotrophic factor (BDNF), the predominant neurotrophin in the adult brain, plays a fundamental role in regulating hippocampal synaptic plasticity and memory consolidation [12,13]. Notably, BDNF levels are altered in both the brain and periphery of AD patients, suggesting its dysfunction in the pathogenesis of the disease [14,15]. Consequently, restoring physiological BDNF levels represents a promising therapeutic strategy to mitigate the synaptic and neuronal loss underlying cognitive decline in AD.

ADSCs do not normally secrete BDNF [16,17], although under certain conditions they may be induced to do



Copyright: © 2026 The Author(s). Published by IMR Press.
This is an open access article under the CC BY 4.0 license.

Publisher's Note: IMR Press stays neutral with regard to jurisdictional claims in published maps and institutional affiliations.

so [12,18–20]. We therefore reasoned that genetically engineering ADSCs to become a localized, long-term source of BDNF could constitute a more effective strategy to counteract both synaptic failure and pathology progression simultaneously. To test this premise, we transfected ADSCs with a BDNF-expressing lentivirus to explore the possibility that this manipulation would enhance their therapeutic potential. The modified ADSCs were transplanted into the dorsal hippocampus of APPswe/PS1dE9 (APP/PS1) mice. Six months after transplantation, we assessed the survival and spatial distribution of BDNF-ADSCs within the hippocampus, their effects on the expression of BDNF and neprilysin-2 (NEP-2; a neprilysin homolog and a key β -amyloid degrading enzyme) [21,22], potential effects on dendritic architecture by examining the pattern of microtubule associated protein 2 (MAP2) expression, and amyloid plaque load. NEP-2; a neprilysin homolog and a key β -amyloid degrading enzyme

2. Materials and Methods

2.1 Animals

Male APP/PS1 mice and C57/BL6J wild-type mice were purchased from Guangdong Medical Laboratory Animal Center (Foshan, Guangdong, China). Mice were maintained under *ad libitum* feeding conditions with free access to a standard laboratory diet and water. Neonatal C57/BL6J mice, raised at the Hainan Research Institute of Medicine, were used to obtain ADSCs. The experimental mice were divided into three groups (12/gp): (a) wild-type controls (C57/BL6J) and (b) APP/PS1 mice that received either BDNF-ADSCs or (c) sham surgery. All experimental procedures were initiated when mice reached 7 mo, and were conducted in compliance with the ARRIVE guidelines 2.0.

2.2 Isolation and Culture of ADSCs

According to a previously described method [23], ADSCs were obtained from the epididymal fat of 2–3-week-old male C57/BL6J mice. Briefly, the adipose tissue was digested with 0.1% collagenase type I (BS-163, Biosharp, Shanghai, China) at 37 °C for 1 h, followed by mechanical dissociation and centrifugation at 800 \times g for 15 min. The pellet was then re-suspended, filtered through a 70- μ m strainer (BS-70-CS, Biosharp), and cultured in complete Dulbecco's modified eagle medium nutrient mixture F-12 (DMEM/F12) (11320033, Thermo Fisher Scientific, Waltham, MA, USA) medium (supplemented with 10% fetal bovine serum (FBS) (A5669701, Thermo Fisher Scientific) and 1% penicillin/streptomycin [15140122, Thermo Fisher Scientific]) at 37 °C with 5% CO₂. The medium was replaced after 24 h to remove nonadherent cells, and the adherent ADSCs were subsequently expanded. All primary cells were validated for their identity by surface marker analysis and tested negative for mycoplasma.

2.3 Flow Cytometry Assays for Cell Surface Antigens

Third passage (P3) ADSCs were harvested, fixed in 75% ethanol on ice, and washed. After filtering, 1 \times 10⁶ cells were stained with fluorescein isothiocyanate (FITC)/phycoerythrin (PE)/phycoerythrin-cyanine 7 (PE-Cy7)-conjugated antibodies against cluster of differentiation (CD)73 (Cat. No. 127205, BioLegend, San Diego, CA, USA), CD105 (Cat. No. 120407, BioLegend), CD90 (ab33694, Abcam, Cambridge, UK), CD34 (ab323757, Abcam), CD45 (Cat. No. 202207, BioLegend), and human leukocyte antigen-DR (HLA-DR) (ab1182, Abcam) for flow cytometry. Phycoerythrin-conjugated immunoglobulin G (PE-IgG) served as an isotype control. The expression of CD surface antigens was analyzed using flow cytometry (BD Biosciences, Franklin Lakes, CA, USA). To functionally characterize their differentiation capacity, ADSCs were subjected to induction protocols for osteogenic, adipogenic, and chondrogenic fates. The resulting phenotypic changes were detected through standard histological methods, employing Alizarin Red S (RAXMA-90021, OriCell, Suzhou, Jiangsu, China), Oil Red O (RAXMA-90031, OriCell), and Alcian Blue (RAXMA-90041, OriCell) staining for the respective lineages [23].

2.4 BDNF-Expressing Lentivirus Preparation and Transduction

A BDNF-encoding lentivirus was produced by co-transfecting 293T cells with plasmids pSPAX2 and pMD2G using LipoFiter™ (KS-TRLF-200/1000, LipoFiter, Shanghai, China). The viral supernatant was collected, filtered, and concentrated by ultracentrifugation. ADSCs were transduced with the lentivirus (Genomeditech, Shanghai, China) at a multiplicity of infection (MOI) of 40 in the presence of 5 μ g/mL polybrene (40804ES76, Yeasen, Shanghai, China), and stable clones were selected with puromycin (ST551, Beyotime, Shanghai, China) over 3 weeks. BDNF expression was confirmed by western blot and immunocytochemistry. The 293T cell line used in this study was obtained from Wanwu Biotechnology (Delf-10618, Hefei, Anhui, China). All cell lines were validated by routine PCR assay and tested negative for mycoplasma.

2.5 BDNF-ADSC Transplantation

APP/PS1 mice were anesthetized using isoflurane (PHR2874, Merck KGaA, Darmstadt, Germany) (3–4% induction, 1.5–2% maintenance) and placed in a stereotaxic frame (RWD Life Science, Shanghai, China). The skull surface was exposed and either 2 μ L of the DMEM/F12 vehicle or 1 \times 10⁶ BDNF-ADSCs suspended in 2 μ L DMEM/F12 were injected bilaterally into the anterior hippocampus using the following coordinates: 1.0 mm posterior to the bregma, \pm 1.0 mm from midline, and 2.0 mm ventral to skull surface. To prevent backflow, the injection needle was left in place for 5 min post-injection, facilitating adequate diffusion of the solution into the local tissue. The injection

needle was then removed and the wound was closed. After surgery, the mice were maintained under thermal support until full recovery from anesthesia, after which they were returned to their home cages.

2.6 Tissue Preparation

After a survival interval of 180 days, mice were deeply anesthetized with 5% isoflurane and euthanized by cervical dislocation. For immunohistochemical studies, 6 mice from each of the three groups (C57/BL6J control, APP/PS1 sham, APP/PS1 ADSC) were perfused intracardially with phosphate buffered saline (PBS) (pH 7.4), followed by perfusion with 4% paraformaldehyde (12352100, SigmaAldrich, St. Louis, MO, USA) in PBS at 4 °C. After overnight post-fixation at 4 °C, the harvested brains were cryoprotected by immersion in a 30% sucrose-PBS solution. After equilibration, serial 40-μm coronal sections were obtained using a Leica CM1900 freezing microtome (Leica Biosystems, Nussloch, Germany) and stored in a cryoprotectant solution (C0171A, Beyotime) [24] at 4 °C for subsequent processing.

For western blot analysis, the remaining 6 mice/gp were transcardially perfused with ice-cold PBS. Following rapid extraction, the brains were placed on a pre-chilled plate for immediate hippocampal dissection. The isolated hippocampal tissue was snap-frozen and maintained at -80 °C until subsequent protein analysis.

2.7 Immunohistochemistry

Tissue sections were treated with 1% H₂O₂/PBS for 30 min, followed by 1 h blocking with 5% normal goat serum containing 0.3% triton X-100 (ST1723, Beyotime). Sections were then co-incubated overnight at 4 °C with primary antibodies against BDNF (1:1000, ab108319, Abcam), Flag-Tag (1:1000, ab205606, Abcam), MAP2 (1:50,000, ab5392, Abcam), and β-amyloid (6E10, 1:200, MA5-51794, Thermo Fisher Scientific). After PBS washes, sections were incubated for 2 h at 26 °C with a mixture of fluorescent secondary antibodies (Cy3- [1:500, 771412ES60, Yeasen], Alexa Fluor 647- [1:500, 96500ES25, Yeasen], and Alexa Fluor 488- [1:200, GB25303, Servicebio, Wuhan, Hubei, China]), followed by 4,6-diamidino-2-phenylindole (DAPI) (G1012, Servicebio) counterstaining. Finally, sections were mounted and imaged using an Olympus FV1000 (Olympus Corporation, Tokyo, Japan) confocal microscope. 6E10-positive plaques in hippocampal regions were quantified per section for each animal.

2.8 Western Blot Analysis

Protein extracts from ADSCs and hippocampal tissues were prepared using radioimmunoprecipitation assay (RIPA) lysis buffer (G2002, Servicebio) supplemented with protease and phosphatase inhibitors (Roche; 04906845001, Roche Diagnostics, Rotkreuz, Switzerland). Hippocampal

samples from 6 mice/gp were pooled before homogenization. Lysates were centrifuged at 14,000 rpm for 15 min at 4 °C, and supernatants were collected for protein concentration determination with a bicinchoninic acid (BCA) (P0010, Beyotime) assay. Proteins (50 μg per lane) were separated on 10% sodium dodecyl sulfate-polyacrylamide gel electrophoresis (SDS-PAGE) gels (P0012AC, Beyotime) and transferred to poly vinylidene fluoride (PVDF) membranes (IPVH00010, Merck Millipore, Darmstadt, Germany). After blocking, membranes were incubated overnight at 4 °C with the following primary antibodies in tris-buffered saline with tween-20 (TBST) (G0004, Servicebio): BDNF (1:1000, ab108319, Abcam), NEP-2 (1:400, BS-11102R, Bioss Antibodies, Beijing, China). β-Actin (GB15003, Servicebio) served as the loading control. Horseradish peroxidase (HRP)-conjugated secondary antibodies (1:10,000, GB23303, Servicebio) were applied, and band signals were detected using a tanon 5500 imaging system (Shanghai Tanon Science & Technology, Shanghai, China). Densitometric data were normalized to β-actin, with the control group set as 1. All experiments were performed in triplicate, and results are presented as mean ± standard error of the mean (SEM).

2.9 Statistical Analyses

All data are presented as mean ± SEM. Data analyses were performed using Prism 9.5 software (GraphPad Software, La Jolla, CA, USA). The normality of the data distribution for each group was assessed using the Shapiro-Wilk test. Homogeneity of variances was confirmed using the Brown-Forsythe test. After confirming that the data met the assumptions of normality and homogeneity of variances, differences between multiple means were analyzed by analysis of variance (ANOVA) with subsequent post-hoc tests where appropriate. Differences between two means were analyzed using two-tailed *t*-tests. Statistical significance was defined as *p* ≤ 0.05. Where applicable, greater levels of significance are denoted as ***p* < 0.01 and ****p* < 0.001.

3. Results

3.1 Cell Surface Antigens on ADSCs

Flow cytometric analysis of P3 ADSCs confirmed a characteristic mesenchymal surface phenotype. Surface-marker profiling revealed that the cells exhibited strong positivity for the characteristic mesenchymal markers (CD73, CD90, CD105) and were negative for hematopoietic markers (CD34, CD45, HLA-DR) (Fig. 1A). This marker profile, consistent with published data [14], verified the successful isolation of a homogeneous population of mesenchymal stem cells, with minimal contamination from endothelial cells or other non-mesenchymal stromal cells (MSC) types. To assess their multipotency, ADSCs were subjected to specific induction protocols to promote their commitment to osteogenic, adipogenic, and chondro-

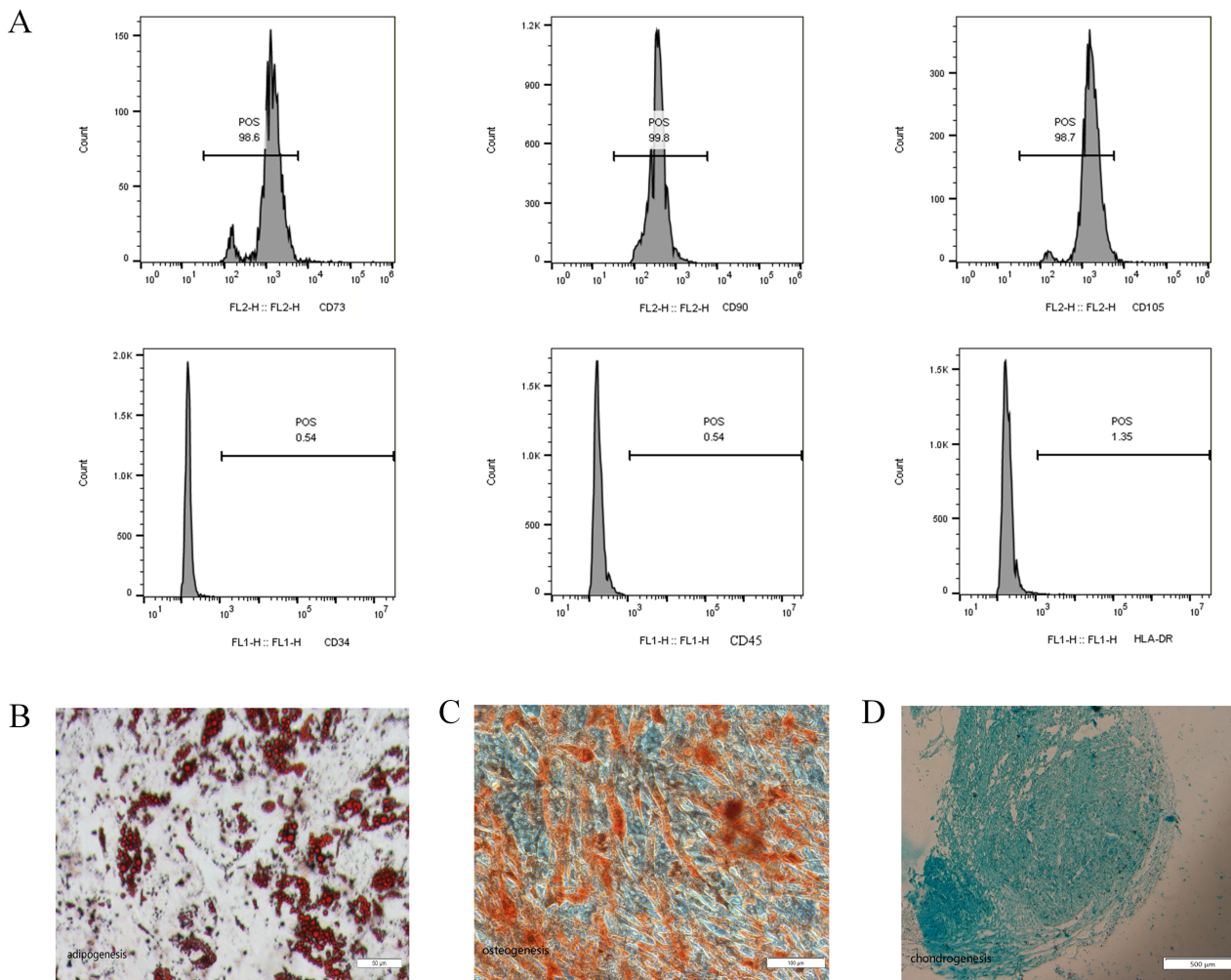


Fig. 1. Cell-surface antigens of ADSCs detected by flow cytometry. (A) Representative results of flow cytometry analysis showed that ADSCs expressed CD73, CD90 and CD105. Bottom: in contrast, almost no expression of the hematopoietic lineage markers CD34, CD45 and HLA-DR was detected. (B) After induction of adipogenic differentiation, the cells showed positive staining for Oil Red O. Scale bar = 50 μ m. (C) After induction of osteogenic differentiation, the cells showed positive staining for Alizarin red. Scale bar = 100 μ m. (D) After induction of chondrogenic differentiation, the cells showed positive staining for Alcian Blue. Scale bar = 500 μ m. (n = 3). ADSCs, adipose-derived stem cells; HLA-DR, human leukocyte antigen-DR; CD, cluster of differentiation; FL1-H, fluorescence channel 1- height; FL2-H, fluorescence channel 2- height; POS, positive.

genic lineages. Successful differentiation was confirmed by lineage-specific staining: Alizarin Red S for calcium deposits in osteocytes, Oil Red O for lipid vacuoles in adipocytes, and Alcian Blue for sulfated proteoglycans in chondrocytes (Fig. 1B–D).

3.2 Exogenous BDNF DNA in ADSCs After Lentiviral Transfection

Successful transduction was confirmed by detecting ZsGreen fluorescence in ADSCs under an inverted microscope at 72 h, indicating expression of the respective exogenous genes (human B-lymphotropic virus [HBLV]-ZsGreen or HBLV-BDNF-flag-ZsGreen). ZsGreen was highly expressed in both cases (Fig. 2A–C). The expression of BDNF protein was confirmed by western blot analysis

using total protein extracts from ADSCs transduced with HBLV-BDNF-flag-ZsGreen, with controls including both untransduced cells and HBLV-ZsGreen-transduced cells. The BDNF-flag-ZsGreen fusion protein was specifically detected at its predicted size via anti-flag western blot in the relevant group, confirming successful expression, whereas control groups showed no signal (Fig. 2D). Immunocytochemistry studies verified that BDNF was expressed in HBLV-BDNF-flag-ZsGreen transfected ADSCs (Fig. 2E).

3.3 Survival and Distribution of BDNF-ADSCs

BDNF-ADSCs were transplanted bilaterally into the anterior hippocampus of 7-mo-old APP/PS1 mice, and analysis was performed 6 mo after transplantation. To investigate the survival and distribution of transplanted

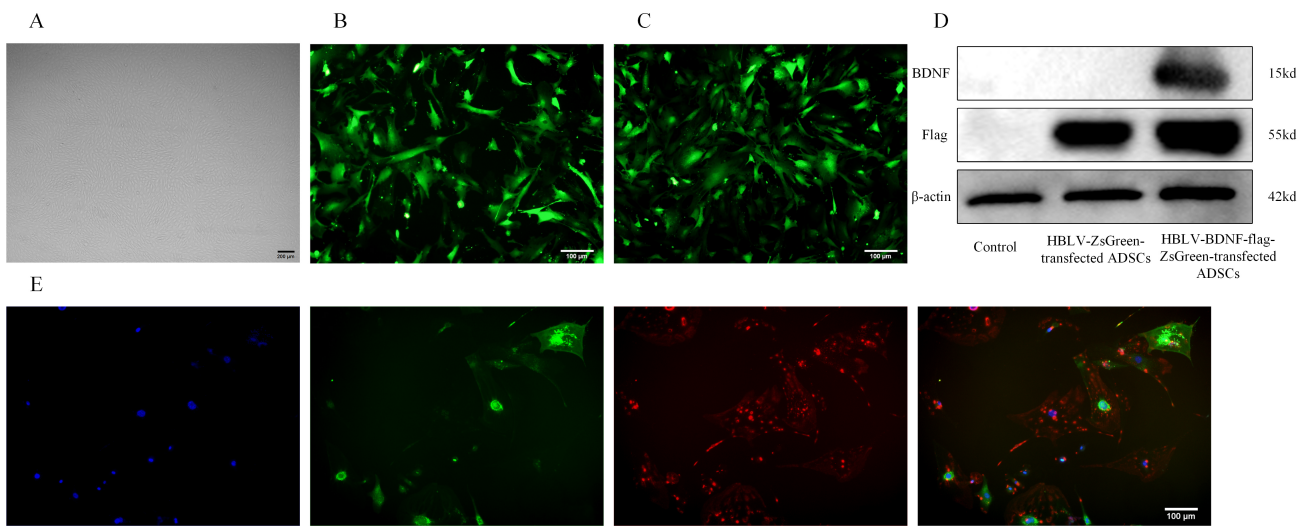


Fig. 2. Expression of exogenous DNA in ADSCs after lentiviral transduction. (A) Representative images of ADSCs. Scale bar = 200 μ m. (B) HBLV-ZsGreen-transfected ADSCs were observed under fluorescence microscope. Transfection success was estimated at >90% (n = 3). (C) Similar results were seen for HBLV-BDNF-flag-ZsGreen-transfected ADSCs observed under fluorescence (n = 3). Scale bars for (B,C): 100 μ m. (D) Western blot demonstrating that BDNF and Flag proteins were not present in non-transfected cells, but were seen in HBLV-ZsGreen-transfected ADSCs and HBLV-BDNF-flag-ZsGreen-transfected ADSCs. All western blot experiments were repeated three times with consistent results. Full-length blots/gels are presented in **Supplementary Fig. 1**. (E) Immunohistochemistry showing an example of the expression of BDNF in HBLV-BDNF-flag-ZsGreen-transfected ADSCs (n = 3). Red = BDNF; green = ZsGreen. Scale bar: 100 μ m. BDNF, brain-derived neurotrophic factor; HBLV, human B-lymphotropic virus.

BDNF-ADSCs the mice were euthanized and coronal sections containing the anterior–posterior axis of the hippocampus were examined using a confocal microscope. As expected, no BDNF-ADSCs were detected in the AD sham group and the wild type (WT) control group (data not shown). Engrafted BDNF-ADSCs were found within and surrounding the retrosplenial cortex, but most cells were seen in stratum oriens and filed CA1 hippocampus (CA1) stratum pyramidale in the hippocampus. Notably, BDNF-ADSCs were seen well caudal to the injection site, indicating that they had migrated during the survival period (Fig. 3).

3.4 BDNF-ADSC Transplantation Increased BDNF and NEP-2 Levels in the Hippocampus

Previous study has shown that the neurotrophin BDNF plays a key role in synaptic plasticity [18]. NEP-2 is an important $\text{A}\beta$ -degrading enzyme. Therefore, we examined BDNF and NEP-2 expression in the hippocampus of APP/PS1 mice 6 mo after BDNF-ADSC transplantation. BDNF and NEP-2 protein expression levels were assessed by western blot (Fig. 4). At 13 months of age, APP/PS1 mice (vehicle-injected Shams) exhibited lower hippocampal protein levels of both BDNF and NEP-2 compared with C57/BL6J controls. All mice were euthanized under 5% isoflurane anesthesia followed by cervical dislocation. However, reduced levels of the two proteins were not seen in APP/PS1 mice that had received BDNF-ADSC cell injections.

3.5 Engrafted BDNF-ADSCs Alter Patterning of Dendritic MAP2 Expression in the Hippocampus

Degradation of dendritic cytoarchitecture is a hallmark of AD, and is reflected in reductions in MAP2 protein levels and patterning in mouse models of the disease [25,26]. Compared to the control group (Fig. 5A), MAP2 staining in hippocampal area CA1 dendrites in 13-mo-old APP/PS1 mice revealed a shortened dystrophic pattern, indicating that microtubule structure was disrupted (Fig. 5B). In contrast, in mice that had received BDNF-ADSC injections, MAP2-stained dendrites were elongated and more densely distributed, similar to what was seen in control C57/BL6J mice (Fig. 5C).

3.6 Transplanted BDNF-ADSCs Reduce $\text{A}\beta$ Plaque Burden in Hippocampus

Immunofluorescence staining was performed on brain sections using the 6E10 anti- $\text{A}\beta$ primary antibody. Amyloid-positive plaques were counted in sections through the hippocampus. Average plaque counts per section were significantly lower in mice that had received BDNF-ADSCs than in vehicle-injected sham mice (Fig. 6).

4. Discussion

This study investigated whether transplantation of BDNF-ADSCs would attenuate hippocampal neuronal pathology in APP/PS1 mice, an established model of AD. We used a novel combinatorial strategy by genetically en-

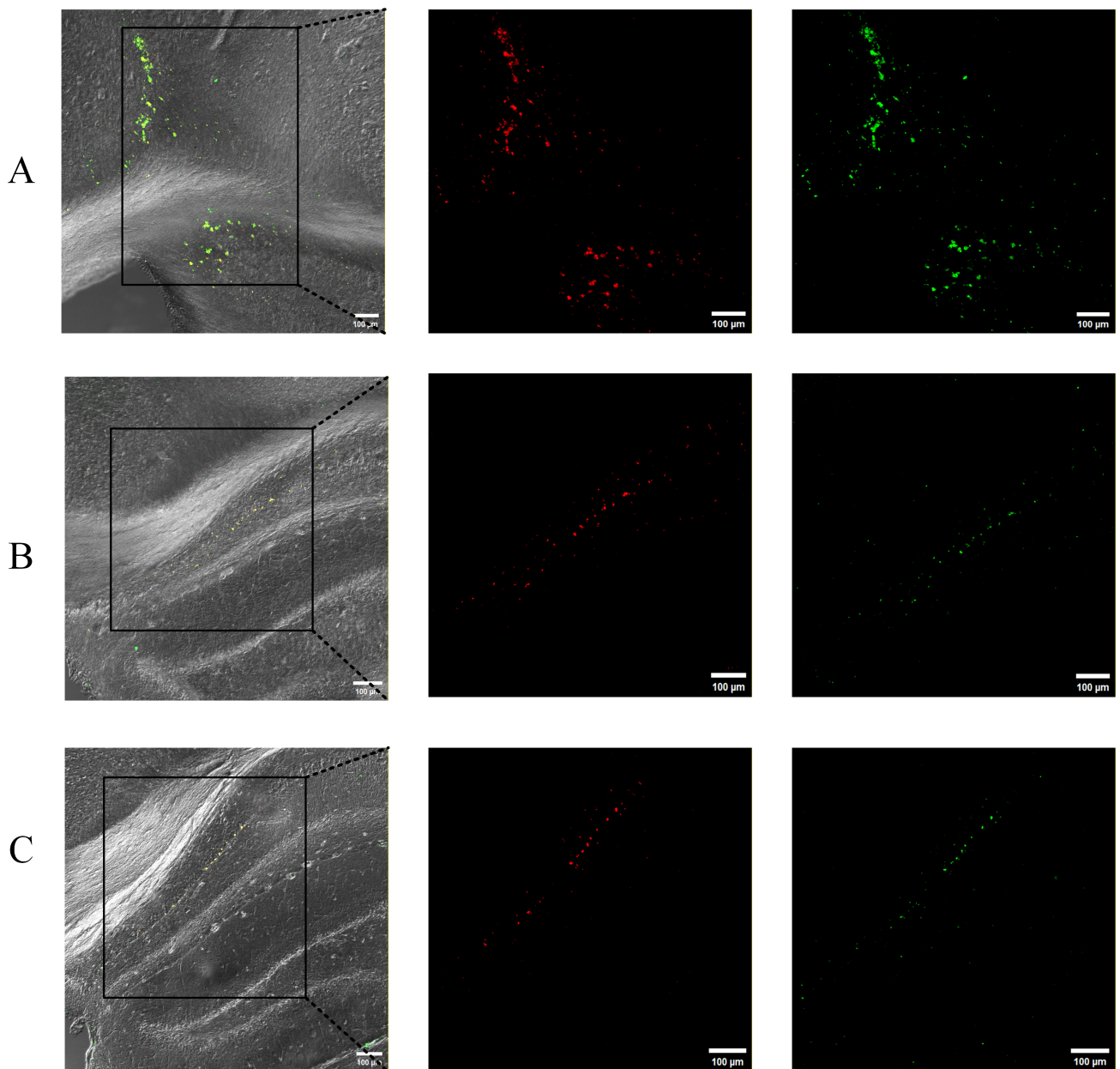


Fig. 3. Representative distribution of transplanted BDNF-ADSCs in the hippocampus of mice. ZsGreen (Green) was used to label the BDNF-ADSCs, Cy3 (Red) was used to label the Flag expression. Each panel displays, from left to right: low-magnification image with higher power area shown in subsequent panels. On the far right are illustrations of the coronal section at which the image was taken. In (A), labeled cells are present in the retrosplenial cortex as well as in the hippocampus. In (B,C), labeled cells are seen in the medial CA1 pyramidal cell layer. Coronal sections shown are, from bregma: -0.94 mm (A); -1.46 mm (B); -1.70 (C); scale bar = 100 μ m; n = 6.

gineering ADSCs to overexpress BDNF through lentiviral transduction. We found that BDNF-ADSCs survived in the hippocampus for 6 mo after transplantation, and appeared to migrate a substantial distance from the injection site. BDNF-ADSC transplantation significantly increased BDNF and NEP-2 expression in treated mice. Moreover, the dendrites of hippocampal neurons, as illustrated by MAP2 staining, were longer and more densely distributed than in sham mice.

Postmortem histopathological analyses of AD patients have demonstrated significant neuronal loss in key brain regions, including the cortex and hippocampus [27,28]. By repopulating lost cells and exerting protective effects, cell-based therapies may mitigate the progression of neurodegenerative diseases [6]. Stem cells have been reported to be short-lived in the brain, in some cases surviving less than one month after transplantation [29]. Therefore, the therapeutic benefits of stem-cell transplantation may be me-

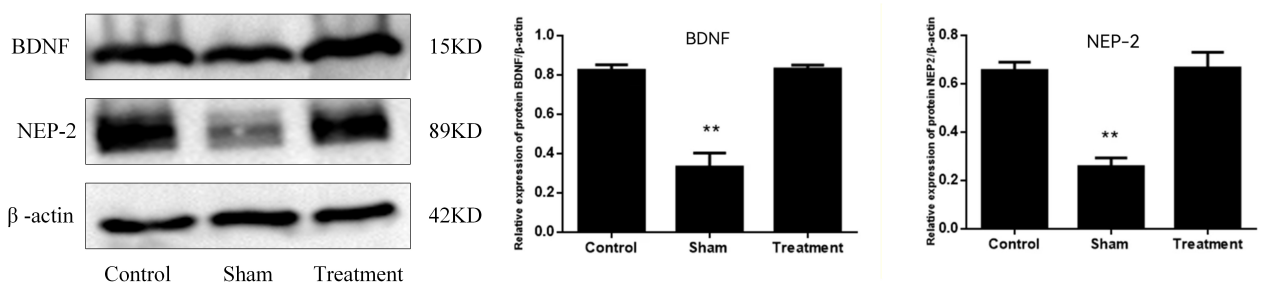


Fig. 4. BDNF-ADSC transplantation normalized BDNF and NEP-2 protein levels in the hippocampus of 13-month-old APP/PS1 mice. Levels of the two proteins were significantly lower in Sham mice than in comparably aged C57/BL6J controls, but treated mice had protein levels that were not different from controls. Data are presented as mean \pm SEM (standard error of the mean, $n = 6/\text{gp}$; results in bar graph are the average of three replicates). Control: C57/BL6J mice; Sham: APP/PS1 mice that received vehicle; Treatment: APP/PS1 mice that received BDNF-ADSCs. Sample western blots are shown on the left side of the figure. Full-length blots/gels are presented in **Supplementary Fig. 2**. Quantified measurements (normalized to actin) are shown on the right. ** $p < 0.01$ vs. control or treatment groups. NEP-2, neprilysin-2.

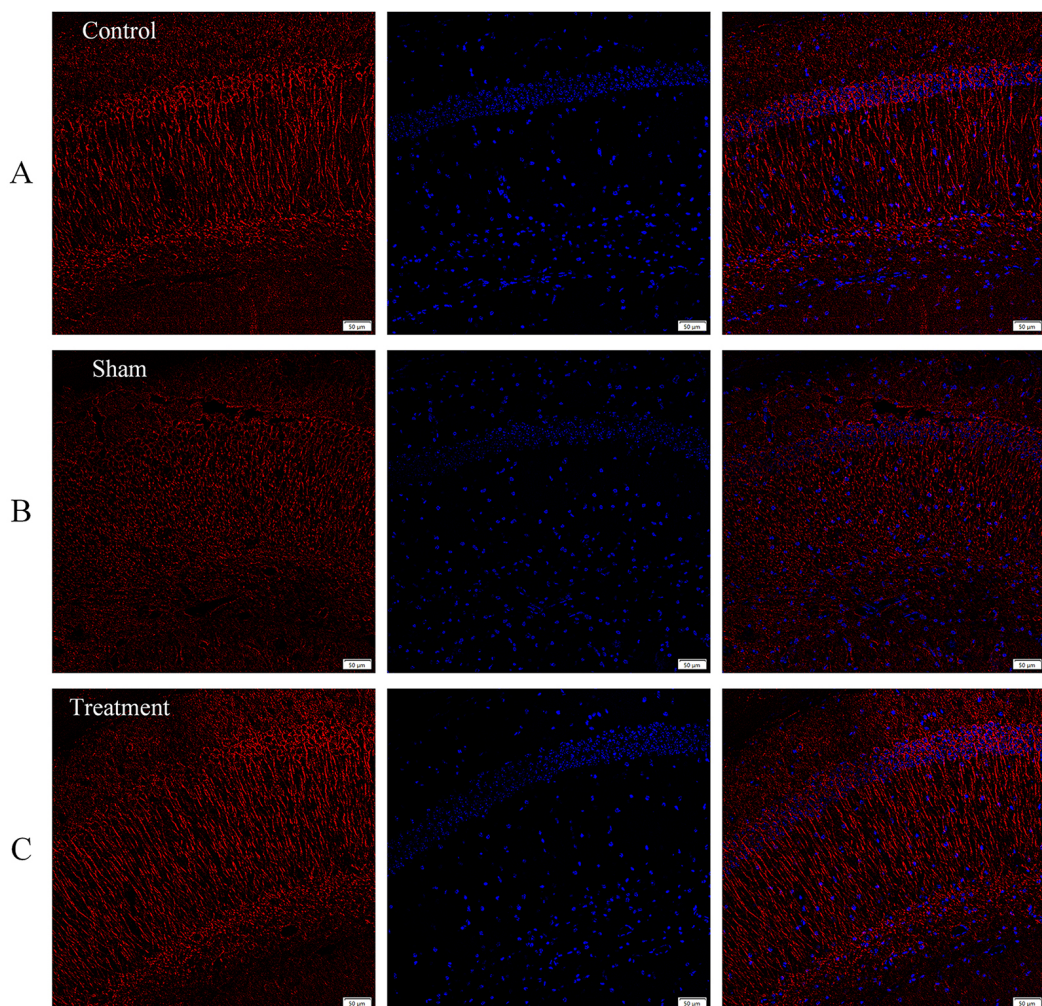


Fig. 5. Engrafted BDNF-ADSCs changed dendritic morphology in the hippocampus of APP/PS1 mice. (A) Immunohistochemical analysis of MAP2 staining in control group. (B) In the sham group, MAP2 stained CA1 dendrites were shortened and dystrophic. (C) In the BDNF-ADSC treatment group, MAP2-stained dendrites appeared elongated and parallel to each other, similar to those seen in the control group. Red: MAP2; blue: 4,6-diamidino-2-phenylindole (DAPI). Scale bar = 50 μm ($n = 6$). MAP2, microtubule associated protein 2.

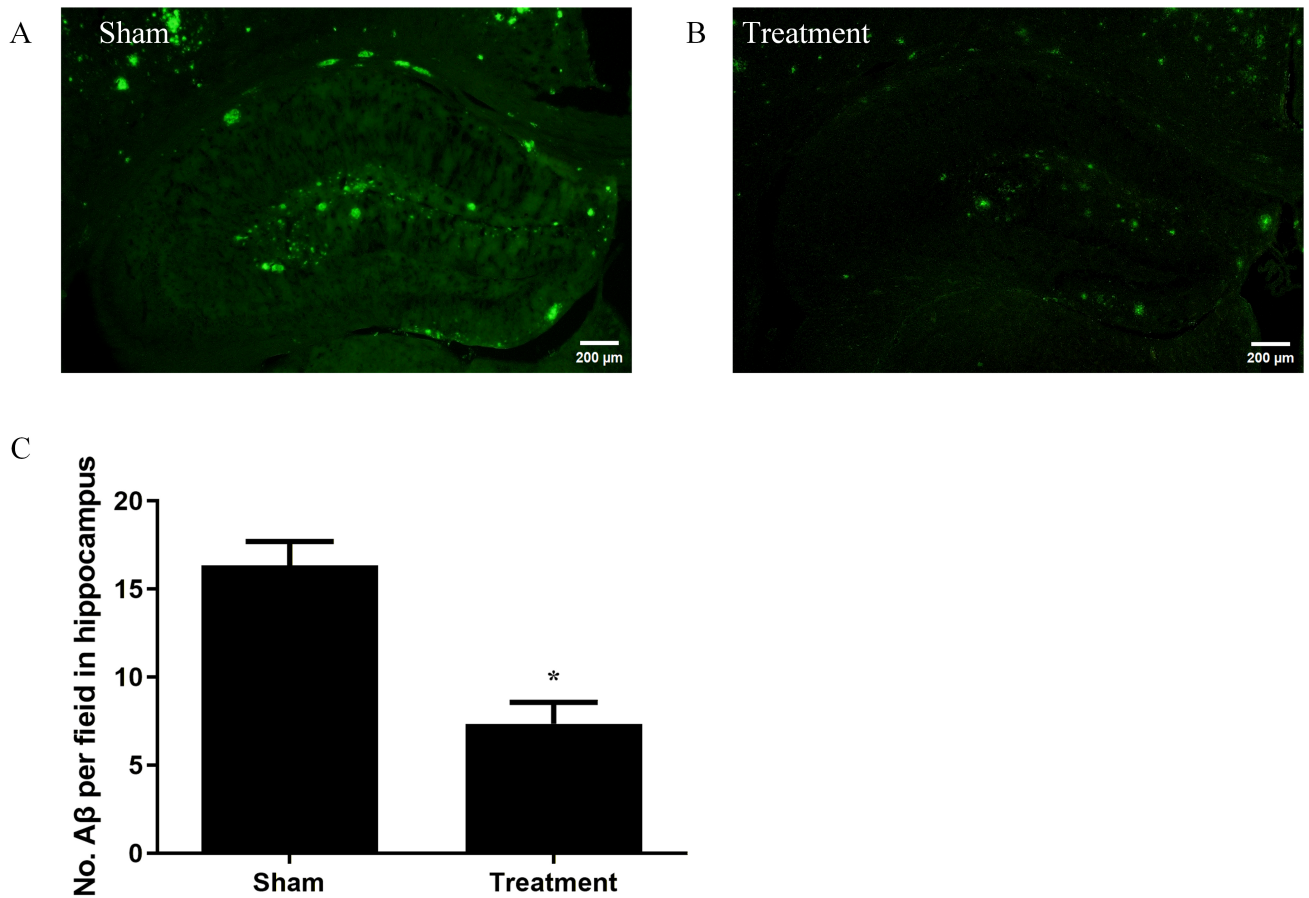


Fig. 6. BDNF-ADSCs diminish A_β plaques in the brains of APP/PS1 mice. Plaques were visualized by fluorescence microscopy using a 6E10 antibody. (A) Representative image of the hippocampus from a sham mouse. (B) Representative image from a mouse that received BDNF-ADSC transplants. (C) Average plaque number per section in the two groups. Counts are the mean \pm SEM of all sections containing the hippocampus from three mice in each group. Scale bar = 200 μ m, $^*p < 0.05$ ($n = 6/\text{gp}$, 3 slices per mouse).

diated primarily by indirect mechanisms activated by the grafted cells, rather than by the direct actions of the cells themselves. For example, the repair mechanisms observed after cell transplantation are primarily mediated by the secretion of paracrine factors from the grafted cells [14,29–32]. The paracrine function of ADSCs involves the release of a broad spectrum of bioactive molecules, including growth factors and exosomes. These secretions enable them to contribute significantly to key biological processes: including the inhibition of apoptosis and inflammation, promotion of angiogenesis, and modulation of immune responses [33–35]. We confirmed that BDNF-ADSCs survive for at least six months after transplantation in the mouse brain. These cells exhibited distribution within the hippocampus and were associated with the amelioration of key pathological features in the APP/PS1 mice. Consistent with this concept, Yu *et al.* [36] demonstrated that genetic modification of ADSCs with vascular endothelial growth factor (VEGF) modified messenger RNA (mod-RNA) transfection enhanced the survival of the transplanted cells. Those engineered ADSCs, when co-transplanted with human fat into a murine model, exhibited elevated proan-

giogenic capacity, which in turn ensured long-term survival of the fat graft [36]. We do not know whether BDNF transfection itself contributed to the longevity of the transplanted cells because we did not do a direct comparison between transfected and nontransfected ADSCs. This is an important topic for future studies.

BDNF is critically involved in key neuronal processes, including promoting neuronal survival, facilitating differentiation, regulating synaptic transmission, and guiding structural plasticity through dendritic remodeling and axon growth [37,38]. Consistently reported low levels of BDNF, at both the mRNA and protein levels, are a hallmark of post-mortem AD brains, particularly affecting the hippocampus and frontal, parietal, and temporal cortices [39,40]. Extensive research has demonstrated that BDNF administration mitigates multiple Alzheimer's-related pathologies in APP transgenic mice, including reducing A_β-mediated neurotoxicity, ameliorating synaptic deficits, and consequently improving cognitive function [15,41–43]. Kim *et al.* [9] showed that transplanted ADSCs did not significantly affect levels of BDNF. However, we successfully elevated hippocampal BDNF protein levels, as intended, by using

our BDNF-transfected ADSC transplantation strategy. The elevated BDNF very likely enhanced the effects of ADSC transplantation. Similar results have been reported by Wu *et al.* [44], who showed that neural stem cells modified to overexpress BDNF showed enhanced efficacy for relieving morphological and behavioral impairments in the Tg2576 mouse model of AD.

NEP and NEP-2 are $A\beta$ -degrading enzymes, which are important regulators of $A\beta$ metabolism [21,45–47]. NEP is dramatically decreased in high-plaque areas in AD brains, and the deficient degradation of $A\beta$ due to NEP deficiency likely contributes to AD pathogenesis [48,49]. ADSC transplantation has recently been shown to exert a neuroprotective effect by mediating $A\beta$ clearance [50,51]. Those authors showed that ADSCs secrete enzymatically active NEP via exosomes, leading to reduced $A\beta$ levels in neuroblastoma cultures. In our study, BDNF-ADSC transplantation dramatically increased the protein expression of NEP-2 in the hippocampus of APP/PS1 mice, and also significantly reduced $A\beta$ plaque load. It is not clear whether elevated levels of BDNF played a role in increasing NEP-2 expression. Kakiya *et al.* [52] reported that, in primary neuronal cultures, BDNF reduced neprilysin activity. However, Safar *et al.* [40] reported that intracranial transplantation of bone-marrow-derived endothelial progenitor cells elevated hippocampal mRNA levels of both *BDNF* and *NEP* in a rat model of AD.

Dendrites, which are crucial for neuronal signal processing, are structurally and functionally impaired by key AD pathogenic agents, including $A\beta$ and tau [53]. Widespread dendritic abnormalities, which emerge early in AD, significantly disrupt neuronal computation by altering dendritic signal integration and spike timing [54]. Our observation of improved dendritic morphology in APP/PS1 mice 6 months after BDNF-ADSC transplantation suggests that hippocampal signal processing should also be improved. In future studies, it will be important to test this idea by evaluating behavioural measures of hippocampal function.

The presence of amyloid plaques, a defining neuropathological hallmark of AD, is a requisite feature of any valid animal model for this condition. Reducing plaque formation or eliminating existing plaques has long been a goal of the development of therapies aimed at forestalling or relieving cognitive symptoms. However, the relationship between amyloid plaques and AD is complex, as it appears that plaque accumulation in the brain occurs many years prior to the appearance of cognitive deficits [55]. Nevertheless, brain amyloid reduction remains a major focus, and is a particular target of new antibody agents [56]. Among other potential benefits, we found that transplantation of BDNF-ADSCs elicited a sustained reduction in hippocampal amyloid plaque load in APP/PS1 mice.

Despite the promising findings, this study had several limitations. First, the absence of a control group involving

wild-type mice transplanted with ADSCs limits our ability to fully dissect the contribution of the disease environment to the observed effects and to rule out non-specific outcomes of the transplantation procedure itself. Furthermore, the most significant functional limitation is the absence of cognitive behavioral assays, which leaves the functional impact of the structural improvements on learning and memory unconfirmed. In addition, although MAP2 immunohistochemistry revealed enhanced dendritic architecture, direct evidence for functional synaptic plasticity, such as from electrophysiological recordings, is lacking. Finally, the observed increases in BDNF and NEP-2, although correlated with reduced plaque load, did not establish a definitive causal mechanism, and future studies using specific pathway inhibitors are needed to elucidate the precise molecular interplay.

5. Conclusions

Our study demonstrated that intra-hippocampal transplantation of BDNF-ADSCs achieved long-term (6 mo) engraftment, elevated expression of BDNF and the amyloid-degrading enzyme NEP, ameliorated dendritic pathology, and reduced $A\beta$ plaque burden. Although these findings position BDNF-ADSC therapy as a promising multi-faceted strategy for Alzheimer's disease, clinical translation necessitates future studies that: (1) delineate the precise molecular mechanisms and relative contributions of BDNF versus NEP-2 to the observed neuroprotection; (2) confirm functional rescue through comprehensive behavioural testing; and (3) establish standardized, scalable protocols for cell manufacturing and delivery that meet regulatory standards for clinical trials.

Availability of Data and Materials

The datasets used and analysed during the current study are available from the corresponding author on reasonable request.

Author Contributions

HZ, GMR: Conceptualization, Supervision, Writing. HZ, LM: Acquisition, Analysis. YZL, YHL, HL, CP: Investigation. All authors contributed to editorial changes in the manuscript. All authors read and approved the final manuscript. All authors have participated sufficiently in the work and agreed to be accountable for all aspects of the work.

Ethics Approval and Consent to Participate

All animal procedures were approved by the Ethics Committee of Hainan Medical University (approval number: HYLL-2021-071#) and were conducted in accordance with the National Institutes of Health Guide for the Care and Use of Laboratory Animals (NIH Publication No. 8023, revised 1978).

Acknowledgment

We acknowledge Hainan Medical University and Public Research Laboratory for providing the research facilities.

Funding

This research was funded by Academic Enhancement Support Program of Hainan Medical University [XSTS2025125]; Hainan Province Science and Technology Special Fund of China [ZDYF2022SHFZ290].

Conflict of Interest

The authors declare no conflict of interest.

Supplementary Material

Supplementary material associated with this article can be found, in the online version, at <https://doi.org/10.31083/JIN46077>.

References

[1] Lane CA, Hardy J, Schott JM. Alzheimer's disease. *European Journal of Neurology*. 2018; 25: 59–70. <https://doi.org/10.1111/ene.13439>.

[2] Jang H, Lee S, Kim YJ, Lee J, Kim SW, Son Y, *et al.* Progressive hippocampal neuroarchitecture changes in the 5×FAD Alzheimer's Disease mouse model. *Journal of Integrative Neuroscience*. 2025; 24: 40831. <https://doi.org/10.31083/JIN40831>.

[3] Macklin L, Griffith CM, Cai Y, Rose GM, Yan XX, Patrylo PR. Glucose tolerance and insulin sensitivity are impaired in APP/PS1 transgenic mice prior to amyloid plaque pathogenesis and cognitive decline. *Experimental Gerontology*. 2017; 88: 9–18. <https://doi.org/10.1016/j.exger.2016.12.019>.

[4] Zhang FQ, Jiang JL, Zhang JT, Niu H, Fu XQ, Zeng LL. Current status and future prospects of stem cell therapy in Alzheimer's disease. *Neural Regeneration Research*. 2020; 15: 242–250. <https://doi.org/10.4103/1673-5374.265544>.

[5] Lo Forno D, Mannino G, Giuffrida R. Functional role of mesenchymal stem cells in the treatment of chronic neurodegenerative diseases. *Journal of Cellular Physiology*. 2018; 233: 3982–3999. <https://doi.org/10.1002/jcp.26192>.

[6] Sugaya K, Vaidya M. Stem Cell Therapies for Neurodegenerative Diseases. *Advances in Experimental Medicine and Biology*. 2018; 1056: 61–84. https://doi.org/10.1007/978-3-319-74470-4_5.

[7] Gimble JM, Katz AJ, Bunnell BA. Adipose-derived stem cells for regenerative medicine. *Circulation Research*. 2007; 100: 1249–1260. <https://doi.org/10.1161/01.RES.0000265074.83288.09>.

[8] Chang KA, Kim HJ, Joo Y, Ha S, Suh YH. The therapeutic effects of human adipose-derived stem cells in Alzheimer's disease mouse models. *Neuro-Degenerative Diseases*. 2014; 13: 99–102. <https://doi.org/10.1159/000355261>.

[9] Kim S, Chang KA, Kim JA, Park HG, Ra JC, Kim HS, *et al.* The preventive and therapeutic effects of intravenous human adipose-derived stem cells in Alzheimer's disease mice. *PLoS ONE*. 2012; 7: e45757. <https://doi.org/10.1371/journal.pone.0045757>.

[10] Ma T, Gong K, Ao Q, Yan Y, Song B, Huang H, *et al.* Intracerebral transplantation of adipose-derived mesenchymal stem cells alternatively activates microglia and ameliorates neuropathological deficits in Alzheimer's disease mice. *Cell Transplantation*. 2013; 22: S113–S126. <https://doi.org/10.3727/096368913X672181>.

[11] Yan Y, Ma T, Gong K, Ao Q, Zhang X, Gong Y. Adipose-derived mesenchymal stem cell transplantation promotes adult neurogenesis in the brains of Alzheimer's disease mice. *Neural Regeneration Research*. 2014; 9: 798–805. <https://doi.org/10.4103/1673-5374.131596>.

[12] Santamaria G, Brandi E, Vitola PL, Grandi F, Ferrara G, Pischiutta F, *et al.* Intranasal delivery of mesenchymal stem cell secretome repairs the brain of Alzheimer's mice. *Cell Death and Differentiation*. 2021; 28: 203–218. <https://doi.org/10.1038/s41418-020-0592-2>.

[13] Karimi-Haghghi S, Chavoshinezhad S, Safari A, Razeghian-Jahromi I, Jamhiri I, Khodabandeh Z, *et al.* Preconditioning with secretome of neural crest-derived stem cells enhanced neurotrophic expression in mesenchymal stem cells. *Neuroscience Letters*. 2022; 773: 136511. <https://doi.org/10.1016/j.neulet.2022.136511>.

[14] Harun ZZ, Abdul Azhar A, Kim YJ, Ibrahim FW, Ng MH, Tan JK, *et al.* Modulation of BDNF/TrkB Signalling Pathway in Alzheimer's Disease: Mechanistic Insights and the Role of Stem Cell Therapy. *Biomedicines*. 2025; 13: 2931. <https://doi.org/10.3390/biomedicines13122931>.

[15] Tang S, Luo W, Wu S, Yuan M, Wen J, Zhong G, *et al.* Hippocampus-targeted BDNF gene therapy to rescue cognitive impairments of Alzheimer's disease in multiple mouse models. *Genes & Diseases*. 2025; 13: 101649. <https://doi.org/10.1210/clinem/dgad142>.

[16] Abdanipour A, Tiraihi T, Delshad A. Trans-differentiation of the adipose tissue-derived stem cells into neuron-like cells expressing neurotrophins by selegiline. *Iranian Biomedical Journal*. 2011; 15: 113–121. <https://doi.org/10.6091/ibj.1011.2012>.

[17] Kapur SK, Katz AJ. Review of the adipose derived stem cell secretome. *Biochimie*. 2013; 95: 2222–2228. <https://doi.org/10.1016/j.biochi.2013.06.001>.

[18] Lopatina T, Kalinina N, Karagyaur M, Stambolsky D, Rubina K, Revischin A, *et al.* Adipose-derived stem cells stimulate regeneration of peripheral nerves: BDNF secreted by these cells promotes nerve healing and axon growth de novo. *PLoS ONE*. 2011; 6: e17899. <https://doi.org/10.1371/journal.pone.0017899>.

[19] Tomita K, Madura T, Sakai Y, Yano K, Terenghi G, Hosokawa K. Glial differentiation of human adipose-derived stem cells: implications for cell-based transplantation therapy. *Neuroscience*. 2013; 236: 55–65. <https://doi.org/10.1016/j.neuroscience.2012.12.066>.

[20] Tse KH, Novikov LN, Wiberg M, Kingham PJ. Intrinsic mechanisms underlying the neurotrophic activity of adipose derived stem cells. *Experimental Cell Research*. 2015; 331: 142–151. <https://doi.org/10.1016/j.yexcr.2014.08.034>.

[21] Hafez D, Huang JY, Huynh AM, Valtierra S, Rockenstein E, Bruno AM, *et al.* Neprilysin-2 is an important β -amyloid degrading enzyme. *The American Journal of Pathology*. 2011; 178: 306–312. <https://doi.org/10.1016/j.ajpath.2010.11.012>.

[22] Rofo F, Metzendorf NG, Saubi C, Suominen L, Godec A, Sehlin D, *et al.* Blood-brain barrier penetrating neprilysin degrades monomeric amyloid-beta in a mouse model of Alzheimer's disease. *Alzheimer's Research & Therapy*. 2022; 14: 180. <https://doi.org/10.1186/s13195-022-01132-2>.

[23] Liu B, Kou J, Li F, Huo D, Xu J, Zhou X, *et al.* Lemon essential oil ameliorates age-associated cognitive dysfunction via modulating hippocampal synaptic density and inhibiting acetylcholinesterase. *Aging*. 2020; 12: 8622–8639. <https://doi.org/10.18632/aging.103179>.

[24] Watson RE Jr, Wiegand SJ, Clough RW, Hoffman GE. Use of cryoprotectant to maintain long-term peptide immunoreactivity

and tissue morphology. *Peptides*. 1986; 7: 155–159. [https://doi.org/10.1016/0196-9781\(86\)90076-8](https://doi.org/10.1016/0196-9781(86)90076-8).

[25] Wang YY, Zhou YN, Jiang L, Wang S, Zhu L, Zhang SS, *et al.* Long-term voluntary exercise inhibited AGE/RAGE and microglial activation and reduced the loss of dendritic spines in the hippocampi of APP/PS1 transgenic mice. *Experimental Neurology*. 2023; 363: 114371. <https://doi.org/10.1016/j.expneurol.2023.114371>.

[26] Zhu Q, Zhang N, Hu N, Jiang R, Lu H, Xuan A, *et al.* Neural stem cell transplantation improves learning and memory by protecting cholinergic neurons and restoring synaptic impairment in an amyloid precursor protein/presenilin 1 transgenic mouse model of Alzheimer's disease. *Molecular Medicine Reports*. 2020; 21: 1172–1180. <https://doi.org/10.3892/mmr.2020.10918>.

[27] Mountjoy CQ, Roth M, Evans NJ, Evans HM. Cortical neuronal counts in normal elderly controls and demented patients. *Neurobiology of Aging*. 1983; 4: 1–11. [https://doi.org/10.1016/0197-4580\(83\)90048-9](https://doi.org/10.1016/0197-4580(83)90048-9).

[28] Simić G, Kostović I, Winblad B, Bogdanović N. Volume and number of neurons of the human hippocampal formation in normal aging and Alzheimer's disease. *The Journal of Comparative Neurology*. 1997; 379: 482–494. [https://doi.org/10.1002/\(sici\)1096-9861\(19970324\)379:4<482::aid-cne2>3.0.co;2-z](https://doi.org/10.1002/(sici)1096-9861(19970324)379:4<482::aid-cne2>3.0.co;2-z).

[29] Zheng XY, Wan QQ, Zheng CY, Zhou HL, Dong XY, Deng QS, *et al.* Amniotic Mesenchymal Stem Cells Decrease A β Deposition and Improve Memory in APP/PS1 Transgenic Mice. *Neurochemical Research*. 2017; 42: 2191–2207. <https://doi.org/10.1007/s11064-017-2226-8>.

[30] Cai Y, Li J, Jia C, He Y, Deng C. Therapeutic applications of adipose cell-free derivatives: a review. *Stem Cell Research & Therapy*. 2020; 11: 312. <https://doi.org/10.1186/s13287-020-01831-3>.

[31] Lee JK, Schuchman EH, Jin HK, Bae JS. Soluble CCL5 derived from bone marrow-derived mesenchymal stem cells and activated by amyloid β ameliorates Alzheimer's disease in mice by recruiting bone marrow-induced microglia immune responses. *Stem Cells*. 2012; 30: 1544–1555. <https://doi.org/10.1002/stem.1125>.

[32] Prockop DJ. "Stemness" does not explain the repair of many tissues by mesenchymal stem/multipotent stromal cells (MSCs). *Clinical Pharmacology and Therapeutics*. 2007; 82: 241–243. <https://doi.org/10.1038/sj.cpt.6100313>.

[33] Qin Y, Ge G, Yang P, Wang L, Qiao Y, Pan G, *et al.* An Update on Adipose-Derived Stem Cells for Regenerative Medicine: Where Challenge Meets Opportunity. *Advanced Science*. 2023; 10: e2207334. <https://doi.org/10.1002/advs.202207334>.

[34] Zou ML, Liu SY, Sun ZL, Wu JJ, Yuan ZD, Teng YY, *et al.* Insights into the role of adipose-derived stem cells: Wound healing and clinical regenerative potential. *Journal of Cellular Physiology*. 2021; 236: 2290–2297. <https://doi.org/10.1002/jcp.30019>.

[35] Abbaszadeh ME, Esmaili M, Bilabari M, Golchin A. Brain-derived neurotrophic factor (BDNF) as biomarker in stem cell-based therapies of preclinical spinal cord injury models: A systematic review. *Tissue & Cell*. 2025; 95: 102875. <https://doi.org/10.1016/j.tice.2025.102875>.

[36] Yu F, Witman N, Yan D, Zhang S, Zhou M, Yan Y, *et al.* Human adipose-derived stem cells enriched with VEGF-modified mRNA promote angiogenesis and long-term graft survival in a fat graft transplantation model. *Stem Cell Research & Therapy*. 2020; 11: 490. <https://doi.org/10.1186/s13287-020-02008-8>.

[37] Colucci-D'Amato L, Speranza L, Volpicelli F. Neurotrophic Factor BDNF, Physiological Functions and Therapeutic Potential in Depression, Neurodegeneration and Brain Cancer. *International Journal of Molecular Sciences*. 2020; 21: 7777. <https://doi.org/10.3390/ijms21207777>.

[38] Chen L, Qi Z. Analysis of the Regeneration Ability of Adipose-Derived Schwann Cells for Sciatic Nerve Defects. *Annals of Plastic Surgery*. 2025; 95: 63–69. <https://doi.org/10.1097/SAP.0000000000004338>.

[39] Phillips HS, Hains JM, Armanini M, Laramee GR, Johnson SA, Winslow JW. BDNF mRNA is decreased in the hippocampus of individuals with Alzheimer's disease. *Neuron*. 1991; 7: 695–702. [https://doi.org/10.1016/0896-6273\(91\)90273-3](https://doi.org/10.1016/0896-6273(91)90273-3).

[40] Safar MM, Arab HH, Rizk SM, El-Maraghy SA. Bone Marrow-Derived Endothelial Progenitor Cells Protect Against Scopolamine-Induced Alzheimer-Like Pathological Aberrations. *Molecular Neurobiology*. 2016; 53: 1403–1418. <https://doi.org/10.1007/s12035-014-9051-8>.

[41] Kopec BM, Zhao L, Rosa-Molinar E, Siahaan TJ. Non-invasive Brain Delivery and Efficacy of BDNF in APP/PS1 Transgenic Mice as a Model of Alzheimer's Disease. *Medical Research Archives*. 2020; 8: 2043. <https://doi.org/10.18103/mra.v8i2.2043>.

[42] Nagahara AH, Merrill DA, Coppola G, Tsukada S, Schroeder BE, Shaked GM, *et al.* Neuroprotective effects of brain-derived neurotrophic factor in rodent and primate models of Alzheimer's disease. *Nature Medicine*. 2009; 15: 331–337. <https://doi.org/10.1038/nm.1912>.

[43] Enogieru AB, Idemudia OU. Antioxidant activity and upregulation of bdnf in lead acetate-exposed rats following pretreatment with vitamin e. *Comparative Clinical Pathology*. 2025; 34: 97–108. <https://doi.org/10.1007/s00580-024-03628-9>.

[44] Wu CC, Lien CC, Hou WH, Chiang PM, Tsai KJ. Gain of BDNF Function in Engrafted Neural Stem Cells Promotes the Therapeutic Potential for Alzheimer's Disease. *Scientific Reports*. 2016; 6: 27358. <https://doi.org/10.1038/srep27358>.

[45] Marr RA, Hafez DM. Amyloid-beta and Alzheimer's disease: the role of neprilysin-2 in amyloid-beta clearance. *Frontiers in Aging Neuroscience*. 2014; 6: 187. <https://doi.org/10.3389/fnagi.2014.00187>.

[46] Webster CI, Burrell M, Olsson LL, Fowler SB, Digby S, Sandercock A, *et al.* Engineering neprilysin activity and specificity to create a novel therapeutic for Alzheimer's disease. *PLoS ONE*. 2014; 9: e104001. <https://doi.org/10.1371/journal.pone.0104001>.

[47] Maigler KC, Buhr TJ, Park CS, Miller SA, Kozlowski DA, Marr RA. Assessment of the Effects of Altered Amyloid-Beta Clearance on Behavior following Repeat Closed-Head Brain Injury in Amyloid-Beta Precursor Protein Humanized Mice. *Journal of Neurotrauma*. 2021; 38: 665–676. <https://doi.org/10.1089/neu.2020.6989>.

[48] Huang JY, Hafez DM, James BD, Bennett DA, Marr RA. Altered NEP2 expression and activity in mild cognitive impairment and Alzheimer's disease. *Journal of Alzheimer's Disease*. 2012; 28: 433–441. <https://doi.org/10.3233/JAD-2011-111307>.

[49] Al-Kuraishy HM, Al-Gareeb AI, Saad HM, Batiha GES. Long-term use of metformin and Alzheimer's disease: beneficial or detrimental effects. *Inflammopharmacology*. 2023; 31: 1107–1115. <https://doi.org/10.1007/s10787-023-01163-7>.

[50] Katsuda T, Tsuchiya R, Kosaka N, Yoshioka Y, Takagaki K, Oki K, *et al.* Human adipose tissue-derived mesenchymal stem cells secrete functional neprilysin-bound exosomes. *Scientific Reports*. 2013; 3: 1197. <https://doi.org/10.1038/srep01197>.

[51] Al-Kuraishy HM, Sulaiman GM, Al-Gareeb AI, Mohammed HA, Albuhadly AK, Abomughaid MM. Targeting the awry A β pathway in Alzheimer's disease: hype and hurdles. *Inflammopharmacology*. 2025; 33: 5945–5961. <https://doi.org/10.1007/s10787-025-01983-9>.

[52] Kakiya N, Saito T, Nilsson P, Matsuba Y, Tsubuki S, Takei N, *et al.* Cell surface expression of the major amyloid- β peptide (A β)-degrading enzyme, neprilysin, depends on phosphorylation by

mitogen-activated protein kinase/extracellular signal-regulated kinase kinase (MEK) and dephosphorylation by protein phosphatase 1a. *The Journal of Biological Chemistry*. 2012; 287: 29362–29372. <https://doi.org/10.1074/jbc.M112.340372>.

[53] Dorostkar MM, Zou C, Blazquez-Llorca L, Herms J. Analyzing dendritic spine pathology in Alzheimer's disease: problems and opportunities. *Acta Neuropathologica*. 2015; 130: 1–19. <https://doi.org/10.1007/s00401-015-1449-5>.

[54] Buskila Y, Crowe SE, Ellis-Davies GCR. Synaptic deficits in layer 5 neurons precede overt structural decay in 5xFAD mice. *Neuroscience*. 2013; 254: 152–159. <https://doi.org/10.1016/j.neuro.2013.09.016>.

[55] Jack CR, Jr, Knopman DS, Jagust WJ, Petersen RC, Weiner MW, Aisen PS, *et al.* Tracking pathophysiological processes in Alzheimer's disease: an updated hypothetical model of dynamic biomarkers. *The Lancet. Neurology*. 2013; 12: 207–216. [https://doi.org/10.1016/S1474-4422\(12\)70291-0](https://doi.org/10.1016/S1474-4422(12)70291-0).

[56] Haddad HW, Malone GW, Comardelle NJ, Degueure AE, Poliwoda S, Kaye RJ, *et al.* Aduhelm, a novel anti-amyloid monoclonal antibody, for the treatment of Alzheimer's Disease: A comprehensive review. *Health Psychology Research*. 2022; 10: 37023. <https://doi.org/10.52965/001c.37023>.